mathematics

MDPI

Article

Mathematical Analysis of Maxwell Fluid Flow through a Porous Plate Channel Induced by a Constantly Accelerating or Oscillating Wall

Constantin Fetecau [1], Rahmat Ellahi [2,3,*] and Sadiq M. Sait [4]

[1] Section of Mathematics, Academy of Romanian Scientists, 050094 Bucharest, Romania; c_fetecau@yahoo.com
[2] Department of Mathematics & Statistics, Faculty of Basic and Applied Sciences, International Islamic University, Islamabad 44000, Pakistan
[3] Fulbright Fellow, Department of Mechanical Engineering, University of California Riverside, Riverside, CA 92521, USA
[4] Center for Communications and IT Research, Research Institute, King Fahd University of Petroleum & Minerals, Dhahran 31261, Saudi Arabia; sadiq@kfupm.edu.sa
* Correspondence: rellahi@alumni.ucr.edu

Abstract: Exact expressions for dimensionless velocity and shear stress fields corresponding to two unsteady motions of incompressible upper-convected Maxwell (UCM) fluids through a plate channel are analytically established. The porous effects are taken into consideration. The fluid motion is generated by one of the plates which is moving in its plane and the obtained solutions satisfy all imposed initial and boundary conditions. The starting solutions corresponding to the oscillatory motion are presented as sum of their steady-state and transient components. They can be useful for those who want to eliminate the transients from their experiments. For a check of the obtained results, their steady-state components are presented in different forms whose equivalence is graphically illustrated. Analytical solutions for the incompressible Newtonian fluids performing the same motions are recovered as limiting cases of the presented results. The influence of physical parameters on the fluid motion is graphically shown and discussed. It is found that the Maxwell fluids flow slower as compared to Newtonian fluids. The required time to reach the steady-state is also presented. It is found that the presence of porous medium delays the appearance of the steady-state.

Keywords: Maxwell fluid; porous plate channel; unsteady motions; finite Fourier sine transform; exact solutions

Citation: Fetecau, C.; Ellahi, R.; Sait, S.M. Mathematical Analysis of Maxwell Fluid Flow through a Porous Plate Channel Induced by a Constantly Accelerating or Oscillating Wall. *Mathematics* **2021**, *9*, 90. https://doi.org/10.3390/math9010090

Received: 28 November 2020
Accepted: 28 December 2020
Published: 4 January 2021

1. Introduction

The motion of incompressible viscous fluids between parallel plates has been extensively studied due to its multiple applications in engineering and science. Exact solutions for such motions are included in the book of Schlichting [1] and the review papers of Wang [2,3]. Interesting solutions for the unsteady simple Couette flow, the unsteady Poiseuille flow, and the unsteady generalized Couette flow (a superposition of the simple Couette flow over the Poiseuille flow) of the incompressible viscous fluids have been also established by Erdogan [4]. However, the first exact solutions for the velocity field corresponding to motions of the incompressible non-Newtonian fluids, more exactly second grade fluids, between parallel plates seem to be those of Rajagopal [5] and Siddiqui et al. [6] when one of the plates slides or oscillates in its plane. Analytical expressions for the steady-state solutions of two oscillatory motions of incompressible Maxwell fluids through a tube with rectangular or isosceles right triangular cross section have been established by Wang et al. [7] and Sun et al., respectively [8]. Some extensions of previous solutions to fractional Maxwell fluids have been developed by Wenchang et al. [9], Qi and Xu [10], and Qi and Liu [11].

At the same time, the study of such flows through porous media is important in many areas including those in natural sciences and technology. A numerical study of the motion of viscous fluids through plate channels of porous media has been presented by Al-Hadhrami et al. [12], while the steady convection flow between inclined parallel plates has been investigated by Cimpean et al. [13]. The porous effects on the unsteady simple Couette flow of the same incompressible viscous fluids have been approximated by Kesavaiah et al. [14]. Effects of the boundary irregularities on the non-isothermal fluid flow through a thin channel filled with porous medium have been numerically visualized by Marušić-Paloka et al. [15]. In a recent paper, Ehlers [16] proved that, although the classical equations play a central role for motions through porous media, they are valid under certain restrictions while the extended equations are valid for arbitrary cases in their field.

A general study of the unsteady hydromagnetic flows of the viscous fluids between infinite horizontal parallel plates through a porous medium was recently reported by Fetecau and Narahari [17]. Other exact solutions for oscillatory motions of the same fluids between two infinite parallel plates have been obtained by Fetecau and Agop [18] and Danish et al. [19] as limiting cases of some results for fluids with pressure-dependent viscosity. To the best of our knowledge, exact solutions for unsteady motions of the incompressible Maxwell fluids through porous plate channels are rare in the existing literature, although such solutions can be useful for checking the accuracy of the numerical methods which are used to solve more complex motion problems. A recent study of isothermal plane steady flow of incompressible Maxwell fluids through a rectangular slit whose walls are porous has been presented by Ullah et al. [20] using a recursive approach.

The main purpose of this note is to establish exact solutions for two unsteady motions of the incompressible upper-convected Maxwell (UCM) fluids through a porous medium between two infinite horizontal parallel plates under isothermal flow conditions. The fluid motion is induced by the lower plate that slides or oscillates in its plane with the velocities At or $V\sin(\omega t)$, respectively. These solutions, which are determined in a simple way using the finite Fourier sine transform only, can be easily reduced to the similar solutions for viscous fluids performing the same motions. The solutions corresponding to the oscillatory motion are presented as a sum of steady-state and transient components. For validation, the steady-state components of the velocity and the shear stress fields are presented in different forms whose equivalence has been graphically illustrated. Finally, the influence of physical parameters on the fluid motion is graphically depicted and discussed. The required time to reach the steady-state for the oscillatory motion is also determined.

2. Presentation of the Problem

Consider an incompressible UCM fluid at rest in a porous medium between two infinite horizontal parallel plates at distance d apart. The constitutive equations of such a fluid are given by the following relations [21]:

$$\boldsymbol{T} = -p\boldsymbol{I} + \boldsymbol{S}, \tag{1a}$$

$$\boldsymbol{S} + \lambda\left(\frac{d\boldsymbol{S}}{dt} - \boldsymbol{L}\boldsymbol{S} - \boldsymbol{S}\boldsymbol{L}^T\right) = \mu(\boldsymbol{L} + \boldsymbol{L}^T), \tag{1b}$$

where $\boldsymbol{T}$ is the Cauchy stress tensor, $\boldsymbol{S}$ is the extra-stress tensor, $-p\boldsymbol{I}$ is the constitutively indeterminate part of the stress due to the constraint of incompressibility, $\boldsymbol{L} = \text{grad}v$ where v is the velocity vector, λ is the relaxation time and μ is the fluid viscosity.

At $t = 0^+$ the lower plate begins to slide in its plane with the velocity At or to oscillate in the same plane with the velocity $V\sin(\omega t)$. Due to the shear, the fluid gradually moves and we are looking for a velocity field $\boldsymbol{v}$ of the form [21]:

$$v = v(y,t) = u(y,t)\mathbf{e}_x, \tag{2}$$

where $\mathbf{e}_x$ is the unit vector along the x-direction of a convenient Cartesian coordinate system x, y and z. The continuity equation is identically satisfied. In the following we also

assume that the extra-stress tensor $\boldsymbol{S}$, as well as the velocity field v, is a function of y and t only.

Introducing the velocity field given by Equation (2) in the constitutive Equation (1b) and bearing in mind the fact that the fluid was at rest in the initial moment, and therefore:

$$v(y,0) = \mathbf{0},\ \boldsymbol{S}(y,0) = \mathbf{0};\quad 0 \le y \le d, \tag{3}$$

it is easy to prove that the components S_{xz}, S_{yz}, S_{yy} and S_{zz} of $\boldsymbol{S}$ are zero and:

$$\tau(y,t) + \lambda \frac{\partial \tau(y,t)}{\partial t} = \mu \frac{\partial u(y,t)}{\partial y}, \tag{4a}$$

$$\sigma_x(y,t) + \lambda \frac{\partial \sigma_x(y,t)}{\partial t} = 2\lambda \tau(y,t) \frac{\partial u(y,t)}{\partial y}, \tag{4b}$$

where $\tau(y,t) = S_{xy}(y,t)$, $\sigma_x(y,t) = S_{xx}(y,t)$ are the non-trivial components of $\boldsymbol{S}$.

In the absence of a pressure gradient in the flow direction, the balance of linear momentum reduces to the following partial differential equation [22]:

$$\rho \frac{\partial u(y,t)}{\partial t} = \frac{\partial \tau(y,t)}{\partial y} + R(y,t);\ 0 < 0 < d,\quad t > 0, \tag{5}$$

where ρ is the fluid density and $R(y,t)$ is the Darcy's resistance for which such fluids have to satisfy the relation [22]:

$$R(y,t) + \lambda \frac{\partial R(y,t)}{\partial t} = -\frac{\mu \varphi}{k} u(y,t). \tag{6}$$

Here, the constants φ and k are the porosity and the permeability of the porous medium.

Eliminating $\tau(y,t)$ between Equations (4a) and (5) and bearing in mind Equation (6), it results for the dimensional velocity field $u(y,t)$ that the next governing partial differential equation is:

$$\lambda \frac{\partial^2 u(y,t)}{\partial t^2} + \frac{\partial u(y,t)}{\partial t} = \nu \frac{\partial^2 u(y,t)}{\partial y^2} - \frac{\nu \varphi}{k} u(y,t);\quad 0 < y < d,\quad t > 0, \tag{7}$$

where $\nu = \mu/\rho$ is the dynamic viscosity of the fluid.

The appropriate initial and boundary conditions are:

$$u(y,0) = 0,\ \left.\frac{\partial u(y,t)}{\partial t}\right|_{t=0} = 0;\ 0 \le y \le d, \tag{8}$$

$$u(0,t) = At,\ u(d,t) = 0;\ t > 0, \tag{9}$$

for the motion induced by the constantly accelerating lower plate, and:

$$u(0,t) = V \sin(\omega t),\ u(0,t) = 0;\ t > 0, \tag{10}$$

together with the same initial conditions (8) for the motion due to sine oscillations of the same plate in its plane. In the last two relations the acceleration A of the motion, as well as the amplitude V and the frequency ω of the oscillations, is constant.

3. Solution

We use the finite Fourier sine transform to establish exact expressions for the dimensionless velocity and the shear stress fields corresponding to the two different motions of incompressible UCM fluids through a porous medium.

3.1. Flow Due to a Constantly Accelerating Plate

In order to make the proposed model non-dimensional, the following dimensionless variables and functions are established:

$$y^* = y/d,\ t^* = t\ \sqrt[3]{A^2/\nu},\ u^* = u/\ \sqrt[3]{A\nu},\ \tau^* = \tau/(\rho d A),\ \sigma_x^* = \sigma_x/(\rho d A). \tag{11}$$

Using the dimensionless entities from the relations (11) in Equations (7)–(9) and removing the star notation, the next non-dimensional initial and boundary value problem:

$$\mathrm{We}\frac{\partial^2 u(y,t)}{\partial t^2} + \frac{\partial u(y,t)}{\partial t} = \frac{1}{\mathrm{Re}}\frac{\partial^2 u(y,t)}{\partial y^2} - Ku(y,t); \quad 0 < y < 1, \quad t > 0, \tag{12}$$

$$u(y,0) = \left.\frac{\partial u(y,t)}{\partial t}\right|_{t=0} = 0 \quad \text{for} \quad 0 \le y \le 1; \tag{13a}$$

$$u(0,t) = t, \quad u(1,t) = 0 \quad \text{if} \quad t > 0, \tag{13b}$$

for the velocity field $u(y,t)$ is obtained. Into Equation (12), the dimensionless porosity parameter K, the Reynolds number Re and the Weissenberg number We are defined by the equalities:

$$\mathrm{Re} = \frac{Ud}{\nu},\ \mathrm{We} = \frac{\lambda U}{d},\ K = \frac{\varphi\nu\ \sqrt[3]{\nu}}{k\ \sqrt[3]{A^2}}, \tag{14}$$

where $U = d\ \sqrt[3]{A^2/\nu}$ is the characteristic velocity. The two numbers Re and We respectively represent the ratio of internal forces to viscous forces, and the ratio of the relaxation time of the fluid and a characteristic time scale. It is also worth to point out the fact that, in comparison with the Weissenberg number whose values are small enough (the graphical representations of Karra et al. [21] and Housiadas [23] correspond to values of We varying between 0.06 and 10), the range of variation of Re is very large [24] (up to 2.000 in the laminar regime, between 2.000 and 4.000 in the transition regime and greater than 4.000 in the turbulent regime for internal flows). Sometimes, a value of the Reynolds number of 2.100 or even 2.300 is taken into consideration by other authors as the limit for laminar flows.

Dimensionless forms of the relations (4) are:

$$\mathrm{We}\frac{\partial \tau(y,t)}{\partial t} + \tau(y,t) = \frac{1}{\mathrm{Re}}\frac{\partial u(y,t)}{\partial y}, \tag{15a}$$

$$\mathrm{We}\frac{\partial \sigma_x(y,t)}{\partial t} + \sigma_x(y,t) = 2\beta\tau(y,t)\frac{\partial u(y,t)}{\partial y}, \tag{15b}$$

where the constant $\beta = \lambda\ \sqrt[3]{A\nu}/d$. Of course, the corresponding initial conditions are:

$$\tau(y,0) = 0;\ 0 \le y \le 1, \tag{16a}$$

$$\sigma_x(y,0) = 0;\ 0 \le y \le 1. \tag{16b}$$

Multiplying Equation (12) by $\sin(\lambda_n y)$, where $\lambda_n = n\pi$, integrating the result with respect to y between zero and one and using the initial and boundary conditions (13), it results that the finite Fourier sine transform $u_{Fn}(t)$ of $u(y,t)$ has to satisfy the ordinary differential equation:

$$\mathrm{ReWe}\frac{d^2 u_{Fn}(t)}{dt^2} + \mathrm{Re}\frac{du_{Fn}(t)}{dt} + (\lambda_n^2 + K\mathrm{Re})u_{Fn}(t) = \lambda_n t;\ t > 0, \tag{17}$$

with the initial conditions:

$$u_{Fn}(0) = 0,\ \left.\frac{du_{Fn}(t)}{dt}\right|_{t=0} = 0;\ n = 1,2,3\ldots \tag{18}$$

The solution of the Equation (17) with the initial conditions (18), is given by:

$$u_{Fn}(t) = \frac{\lambda_n(\mu_n^2 + \mathrm{Re}r_{2n})}{(r_{2n} - r_{1n})\mu_n^4} e^{r_{1n}t} - \frac{\lambda_n(\mu_n^2 + \mathrm{Re}r_{1n})}{(r_{2n} - r_{1n})\mu_n^4} e^{r_{2n}t} + \frac{\lambda_n}{\mu_n^2}\left(t - \frac{\mathrm{Re}}{\mu_n^2}\right), \tag{19}$$

where $r_{1n}, r_{2n} = \left[-1 \pm \sqrt{1 - 4\mathrm{We}\mu_n^2/\mathrm{Re}}\right]/(2\mathrm{We})$ and $\mu_n^2 = \lambda_n^2 + K\mathrm{Re}$. Consequently, the dimensionless velocity field corresponding to this motion of the incompressible UCM fluids through a porous plate channel is given by the relation:

$$u(y,t) = 2\sum_{n=1}^{\infty}\left[t - \frac{\mathrm{Re}}{\mu_n^2} - \frac{(\mu_n^2 + \mathrm{Re}r_{1n})e^{r_{2n}t} - (\mu_n^2 + \mathrm{Re}r_{2n})e^{r_{1n}t}}{\mu_n^2(r_{2n} - r_{1n})}\right]\frac{\lambda_n \sin(\lambda_n y)}{\mu_n^2}, \tag{20}$$

or equivalently (see the entry three of Table IX in [25]):

$$\begin{aligned} u(y,t) &= (1-y)t - 2tK\mathrm{Re}\sum_{n=1}^{\infty}\frac{\sin(\lambda_n y)}{\lambda_n \mu_n^2} \\ &-2\mathrm{Re}\sum_{n=1}^{\infty}\left[1 + \frac{(\mu_n^2+\mathrm{Re}r_{1n})e^{r_{2n}t} - (\mu_n^2+\mathrm{Re}r_{2n})e^{r_{1n}t}}{(r_{2n}-r_{1n})\mathrm{Re}}\right]\frac{\lambda_n \sin(\lambda_n y)}{\mu_n^4}. \end{aligned} \tag{21}$$

Of course, from Equation (21) it results that the velocity field $u(y,t)$ satisfies all imposed initial and boundary conditions. In the absence of porous effects, it takes the simpler form:

$$u(y,t) = (1-y)t - 2\mathrm{Re}\sum_{n=1}^{\infty}\left\{1 + \frac{(\lambda_n^2 + \mathrm{Re}r_{3n})e^{r_{4n}t} - (\lambda_n^2 + \mathrm{Re}r_{4n})e^{r_{3n}t}}{(r_{4n} - r_{3n})\mathrm{Re}}\right\}\frac{\sin(\lambda_n y)}{\lambda_n^3}, \tag{22}$$

where $r_{3n}, r_{4n} = \left[-1 \pm \sqrt{1 - 4\mathrm{We}\lambda_n^2/\mathrm{Re}}\right]/(2\mathrm{We})$. As expected, making $\mathrm{We} \to 0$ in Equations (21) and (22), we recover the similar solutions corresponding to incompressible Newtonian fluids performing the same motion. Equation (21), for instance, takes the simpler form [17], Equation (29):

$$u_N(y,t) = (1-y)t - 2tK\mathrm{Re}\sum_{n=1}^{\infty}\frac{\sin(\lambda_n y)}{\lambda_n \mu_n^2} - 2\mathrm{Re}\sum_{n=1}^{\infty}\frac{\lambda_n \sin(\lambda_n y)}{\mu_n^4}\left[1 - \exp\left(-\frac{\mu_n^2}{\mathrm{Re}}t\right)\right]. \tag{23}$$

To determine the dimensionless frictional forces per unit area exerted by the fluid on the plates, the corresponding non-trivial shear stress $\tau(y,t)$ has to be known. Introducing the expression of $u(y,t)$ from Equation (21) in (15a) and integrating the respective equation using the initial condition (16a), it results for $\tau(y,t)$ the expression:

$$\begin{aligned} \tau(y,t) &= -\tfrac{t}{\mathrm{Re}} + \tfrac{\mathrm{We}}{\mathrm{Re}}\left[1 - \exp\left(-\tfrac{t}{\mathrm{We}}\right)\right] - 2K\sum_{n=1}^{\infty}\left\{t - \left(\mathrm{We} - \tfrac{\lambda_n^2}{K\mu_n^2}\right)\left[1 - \exp\left(-\tfrac{t}{\mathrm{We}}\right)\right]\right\}\tfrac{\cos(\lambda_n y)}{\mu_n^2} \\ &-\tfrac{2}{\mathrm{Re}}\sum_{n=1}^{\infty}\left\{\tfrac{\mu_n^2+\mathrm{Re}r_{1n}}{\mathrm{We}r_{2n}+1}e^{r_{2n}t} - \tfrac{\mu_n^2+\mathrm{Re}r_{2n}}{\mathrm{We}r_{1n}+1}e^{r_{1n}t}\right\}\tfrac{\lambda_n^2\cos(\lambda_n y)}{(r_{2n}-r_{1n})\mu_n^4} + \tfrac{2}{\mathrm{Re}}\exp\left(-\tfrac{t}{\mathrm{We}}\right) \\ &\times\sum_{n=1}^{\infty}\left\{\tfrac{(\mu_n^2+\mathrm{Re}r_{1n})(\mathrm{We}r_{1n}+1)-(\mu_n^2+\mathrm{Re}r_{2n})(\mathrm{We}r_{2n}+1)}{(r_{2n}-r_{1n})(\mathrm{We}r_{1n}+1)(\mathrm{We}r_{2n}+1)}\right\}\tfrac{\lambda_n^2\cos(\lambda_n y)}{\mu_n^4}. \end{aligned} \tag{24}$$

Making $\mathrm{We} \to 0$, the non-dimensional shear stress corresponding to incompressible Newtonian fluids performing the same motion, as given in [17] if its Equation (30):

$$\tau_N(y,t) = -\frac{t}{\mathrm{Re}} - 2tK\sum_{n=1}^{\infty}\frac{\cos(\lambda_n y)}{\mu_n^2} - 2\sum_{n=1}^{\infty}\frac{\lambda_n^2\cos(\lambda_n y)}{\mu_n^4}\left[1 - \exp\left(-\frac{\mu_n^2}{\mathrm{Re}}t\right)\right], \tag{25}$$

is recovered. Finally, it is worth pointing out the fact that the motion studied here is unsteady and remains unsteady. At large values of the time t, the fluid motion can be well enough described by the long-time solutions:

$$\begin{aligned} u_{Lt}(y,t) &= (1-y)t - 2\mathrm{Re}\sum_{n=1}^{\infty}\left(tK + \frac{\lambda_n^2}{\mu_n^2}\right)\frac{\sin(\lambda_n y)}{\lambda_n \mu_n^2}, \\ \tau_{Lt}(y,t) &= \frac{-t+\mathrm{We}}{\mathrm{Re}} - 2K\sum_{n=1}^{\infty}\left(t - \mathrm{We} + \frac{\lambda_n^2}{K\mu_n^2}\right)\frac{\cos(\lambda_n y)}{\mu_n^2}. \end{aligned} \tag{26}$$

3.2. Flow Due to Sine Oscillations of the Lower Plate

Introducing the next non-dimensional variables, functions and parameter:

$$y^* = y/d, \quad t^* = tV/d, \quad u^* = u/V, \quad \tau^* = \tau/(\rho V^2), \quad \sigma_x^* = \sigma_x/(\rho V^2), \quad \omega^* = \omega d/V, \tag{27}$$

in Equation (7), one obtains the same ordinary differential Equation (12) in which:

$$\mathrm{Re} = \frac{Vd}{\nu}, \ \mathrm{We} = \frac{\lambda V}{d} \quad \text{and} \quad K = \frac{\nu\varphi d}{k\,V}. \tag{28}$$

The initial conditions are given by the same relations (13a) and (13b) while the corresponding boundary conditions are given by the relations:

$$u(0,t) = \sin(\omega t);\ t > 0, \tag{29a}$$

$$u(1,t) = 0;\ t > 0. \tag{29b}$$

Applying again the finite Fourier sine transform to Equation (12) and bearing in mind the boundary conditions (29), one attains the next ordinary differential equation:

$$\mathrm{ReWe}\frac{d^2u_{Fn}(t)}{dt^2} + \mathrm{Re}\frac{du_{Fn}(t)}{dt} + \mu_n^2 u_{Fn}(t) = \lambda_n \sin(\omega t);\ t > 0, \tag{30}$$

with the initial conditions (18). The solution of the ordinary differential Equation (30) with the initial conditions (18) is given by the relation:

$$u_{Fn}(t) = \frac{a_n \sin(\omega t) - \omega\mathrm{Re}\cos(\omega t)}{a_n^2 + (\omega\mathrm{Re})^2}\lambda_n + \frac{\left(a_n + \mathrm{Re}r_{2n}\right)\mathrm{e}^{r_{1n}t} - \left(a_n + \mathrm{Re}r_{1n}\right)\mathrm{e}^{r_{2n}t}}{(r_{2n} - r_{1n})[a_n^2 + (\omega\mathrm{Re})^2]}\omega\lambda_n, \tag{31}$$

where $a_n = \mu_n^2 - \mathrm{ReWe}\omega^2$.

By applying the inverse finite Fourier sine transform to Equation (31), the result is that the dimensionless velocity field $u_s(y,t)$ corresponding to the motion of the incompressible UCM fluids through a porous plate channel induced by sine oscillations of the lower plate in its plane can be presented as a sum, namely:

$$u_s(y,t) = u_{sp}(y,t) + u_{st}(y,t), \tag{32}$$

where

$$u_{sp}(y,t) = 2\sum_{n=1}^{\infty}\frac{a_n \sin(\omega t) - \omega\mathrm{Re}\cos(\omega t)}{a_n^2 + (\omega\mathrm{Re})^2}\lambda_n \sin(\lambda_n y), \tag{33}$$

$$u_{st}(y,t) = 2\omega\sum_{n=1}^{\infty}\frac{\left(a_n + \mathrm{Re}r_{2n}\right)\mathrm{e}^{r_{1n}t} - \left(a_n + \mathrm{Re}r_{1n}\right)\mathrm{e}^{r_{2n}t}}{(r_{2n} - r_{1n})[a_n^2 + (\omega\mathrm{Re})^2]}\lambda_n \sin(\lambda_n y), \tag{34}$$

are its steady-state (permanent or long time) and transient components.

Some time after the initiation of motion, the fluid moves according to the starting solution. After this time, when the transients disappear or can be neglected, the fluid motion is characterized by the steady-state solution. This is the time to reach the steady-state. In practice, it is important for the experimentalists who want to eliminate the transients from their experiments. Graphically, it is the time after which the diagrams of the starting

solution $u_s(y,t)$ overlap on the diagram of its steady-state component $u_{sp}(y,t)$. We shall determine this time for different values of the Weissenberg number We and the porosity parameter K.

Direct computations show that $u_s(y,t)$ given by Equation (32) satisfies the governing Equation (12), the initial conditions (13a) and (13b) and the boundary condition (29b). However, the boundary condition (29a) seems to be unsatisfied. In order to avoid this uncertainty we present the steady-state component $u_{sp}(y,t)$ under the equivalent form:

$$u_{sp}(y,t) = (1-y)\sin(\omega t) + 2\mathrm{Re}\sum_{n=1}^{\infty} \frac{[a_n(\mathrm{We}\omega^2 - K) - \mathrm{Re}\omega^2]\sin(\omega t) - \omega\lambda_n^2\cos(\omega t)}{a_n^2 + (\omega\mathrm{Re})^2} \frac{\sin(\lambda_n y)}{\lambda_n}. \tag{35}$$

Using the steady-state complex velocity $u_p(y,t) = u_{cp}(y,t) + iu_{sp}(y,t)$, where $u_{cp}(y,t)$ is the permanent component of the dimensionless velocity field $u_c(y,t)$ corresponding to the motion induced by cosine oscillations of the lower plate and i is the imaginary unit, it is not difficult to show that $u_{sp}(y,t)$ can be presented in the simpler but equivalent form:

$$u_{sp}(y,t) = \mathrm{Im}\left\{\frac{\mathrm{sh}[(1-y)\sqrt{\gamma}]}{\mathrm{sh}(\sqrt{\gamma})} e^{i\omega t}\right\}; \quad \gamma = \mathrm{Re}(K - \mathrm{We}\omega^2 + i\omega), \tag{36}$$

where "Im" denotes the imaginary part of that which follows. Figure 1, clearly illustrates the equivalence of the two expressions of $u_{sp}(y,t)$ given by Equations (35) and (36).

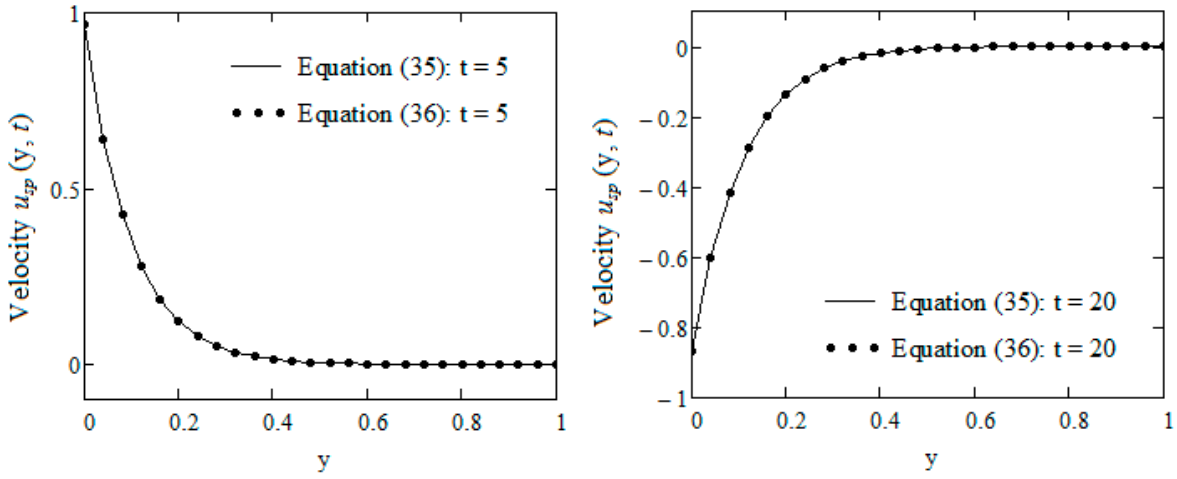

Figure 1. Profiles of the steady-state component $u_{sp}(y,t)$ given by Equations (35) and (36) for $\omega = \pi/12$, $K = 1$, $\mathrm{Re} = 100$ and $\mathrm{We} = 0.7$.

In addition, in the absence of porous effects, expression (36) becomes identical to the solution obtained in ([26] of its Equation (56)).

Furthermore, in the same conditions as before Equations (34) and (35) take the simpler forms:

$$u_{sp}(y,t) = (1-y)\sin(\omega t) + 2\omega\mathrm{Re}\sum_{n=1}^{\infty} \frac{\omega(a_n\mathrm{We} - \mathrm{Re})\sin(\omega t) - \lambda_n^2\cos(\omega t)}{a_n^2 + (\omega\mathrm{Re})^2} \frac{\sin(\lambda_n y)}{\lambda_n}, \tag{37}$$

$$u_{st}(y,t) = 2\omega\sum_{n=1}^{\infty} \frac{(\lambda_n^2 - \mathrm{ReWe}\omega^2 + \mathrm{Re}r_{2n})e^{r_{1n}t} - (\lambda_n^2 - \mathrm{ReWe}\omega^2 + \mathrm{Re}r_{1n})e^{r_{2n}t}}{(r_{2n} - r_{1n})[(\lambda_n^2 - \mathrm{ReWe}\omega^2)^2 + (\omega\mathrm{Re})^2]}\lambda_n\sin(\lambda_n y), \tag{38}$$

while the solutions $u_{Nsp}(y,t)$ and $u_{Nst}(y,t)$ corresponding to the incompressible Newtonian fluids performing the same motion, with or without porous effects, can be immediately obtained by making $\mathrm{We} = 0$ in the corresponding relations.

The non-dimensional shear stress $\tau_s(y,t)$ corresponding to this motion of the incompressible UCM fluids can be determined introducing the expression of $u_s(y,t)$ in Equation (15a) and solving the obtained ordinary differential equation with the initial

condition (16a). The velocity field $u_s(y,t)$, and the shear stress field $\tau_s(y,t)$, as well as the velocity $u_s(y,t)$ can be presented under the form:

$$\tau_s(y,t) = \tau_{sp}(y,t) + \tau_{st}(y,t), \tag{39}$$

whose steady-state and transient components are given by the relations:

$$\tau_{sp}(y,t) = \frac{\omega \mathrm{We}\cos(\omega t) - \sin(\omega t)}{[(\omega \mathrm{We})^2+1]\mathrm{Re}} + 2\sum_{n=1}^{\infty} \frac{(b_n - \mathrm{We}\omega^2\lambda_n^2)\sin(\omega t) - \omega(b_n \mathrm{We} + \lambda_n^2)\cos(\omega t)}{[a_n^2 + (\omega \mathrm{Re})^2][(\omega \mathrm{We})^2+1]}\cos(\lambda_n y), \tag{40}$$

$$\begin{aligned}\tau_{st}(y,t) = {} & \tfrac{2\omega}{\mathrm{Re}}\sum_{n=1}^{\infty} \frac{(a_n+\mathrm{Re}r_{2n})(\mathrm{We}r_{2n}+1)\mathrm{e}^{r_{1n}t} - (a_n+\mathrm{Re}r_{1n})(\mathrm{We}r_{1n}+1)\mathrm{e}^{r_{2n}t}}{(r_{2n}-r_{1n})(\mathrm{We}r_{1n}+1)(\mathrm{We}r_{2n}+1)[a_n^2+(\omega \mathrm{Re})^2]}\lambda_n^2\cos(\lambda_n y) \\ & - \tfrac{2\omega}{\mathrm{Re}}\exp\left(-\tfrac{t}{\mathrm{We}}\right)\sum_{n=1}^{\infty} \frac{(a_n+\mathrm{Re}r_{2n})(\mathrm{We}r_{2n}+1) - (a_n+\mathrm{Re}r_{1n})(\mathrm{We}r_{1n}+1)}{(r_{2n}-r_{1n})(\mathrm{We}r_{1n}+1)(\mathrm{We}r_{2n}+1)[a_n^2+(\omega \mathrm{Re})^2]}\lambda_n^2\cos(\lambda_n y) \\ & - \exp\left(-\tfrac{t}{\mathrm{We}}\right)\left\{\frac{\omega \mathrm{We}}{[(\omega \mathrm{We})^2+1]\mathrm{Re}} - 2\omega\sum_{n=1}^{\infty}\frac{\lambda_n^2+\mathrm{We}b_n}{[a_n^2+(\omega \mathrm{Re})^2][(\omega \mathrm{We})^2+1]}\cos(\lambda_n y)\right\},\end{aligned} \tag{41}$$

where $b_n = (\mu_n^2 - \mathrm{ReWe}\omega^2)(\mathrm{We}\omega^2 - K) - \mathrm{Re}\omega^2$. Taking $y = 1$ into Equations (40) and (41), for instance, the corresponding dimensionless steady-state and transient frictional forces per unit area exerted by the fluid on the stationary plate are immediately obtained.

An equivalent form for the steady-state component $\tau_{sp}(y,t)$ of the dimensionless non-trivial shear stress $\tau_s(y,t)$, namely:

$$\tau_{sp}(y,t) = -\frac{1}{\mathrm{Re}}\mathrm{Im}\left\{\frac{\sqrt{\gamma}}{1+i\omega \mathrm{We}}\frac{\mathrm{ch}[(1-y)\sqrt{\gamma}]}{\mathrm{sh}(\sqrt{\gamma})}\mathrm{e}^{i\omega t}\right\}, \tag{42}$$

can be easily obtained following the same way as for $u_{sp}(y,t)$. The equivalence of the two expressions of $\tau_{sp}(y,t)$ given by Equations (40) and (42) is graphically shown in Figure 2.

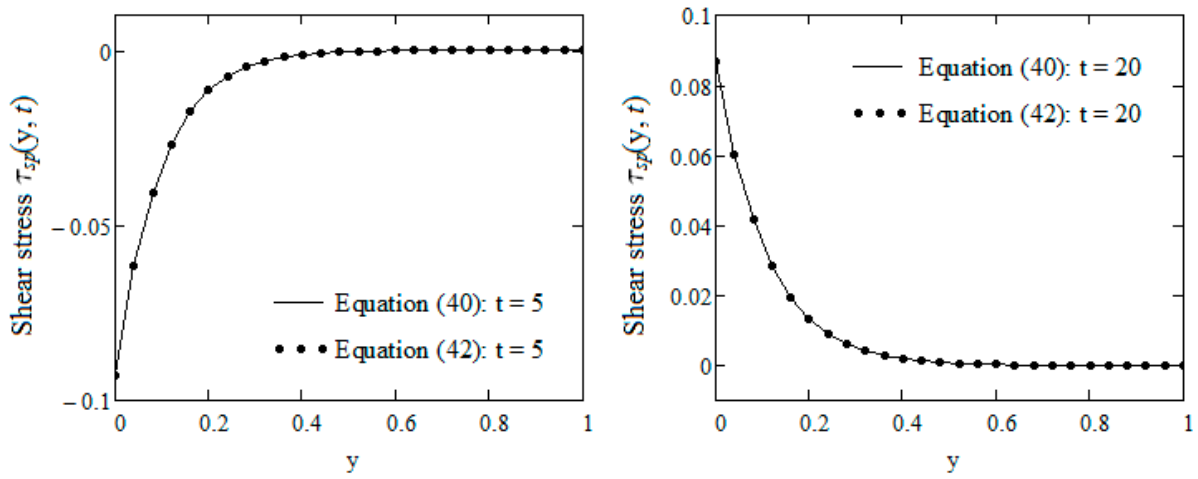

Figure 2. Profiles of the steady-state component $\tau_{sp}(y,t)$ given by Equations (40) and (42) for $\omega = \pi/12$, $K = 1$, $\mathrm{Re} = 100$ and $\mathrm{We} = 0.7$.

Similar solutions corresponding to incompressible Newtonian fluids performing the same motion, namely:

$$u_{Nsp}(y,t) = (1-y)\sin(\omega t) - 2\mathrm{Re}\sum_{n=1}^{\infty}\frac{(K\mu_n^2 + \mathrm{Re}\omega^2)\sin(\omega t) + \omega\lambda_n^2\cos(\omega t)}{(\lambda_n^2 + K\mathrm{Re})^2 + (\omega \mathrm{Re})^2}\frac{\sin(\lambda_n y)}{\lambda_n}, \tag{43}$$

$$u_{Nst}(y,t) = 2\omega \mathrm{Re}\sum_{n=1}^{\infty}\frac{\lambda_n \sin(\lambda_n y)}{(\lambda_n^2 + K\mathrm{Re})^2 + (\omega \mathrm{Re})^2}\exp\left[-\left(\frac{\lambda_n^2}{\mathrm{Re}} + K\right)t\right], \tag{44}$$

$$\tau_{Nsp}(y,t) = -\frac{1}{\mathrm{Re}}\sin(\omega t) - 2\sum_{n=1}^{\infty}\frac{(K\mu_n^2 + \mathrm{Re}\omega^2)\sin(\omega t) - \omega\lambda_n^2\cos(\omega t)}{(\lambda_n^2 + K\mathrm{Re})^2 + (\omega\mathrm{Re})^2}\cos(\lambda_n y), \quad (45)$$

$$\tau_{Nst}(y,t) = 2\omega\sum_{n=1}^{\infty}\frac{\lambda_n^2\cos(\lambda_n y)}{(\lambda_n^2 + K\mathrm{Re})^2 + (\omega\mathrm{Re})^2}\exp\left[-\left(\frac{\lambda_n^2}{\mathrm{Re}} + K\right)t\right], \quad (46)$$

are immediately obtained making $\mathrm{We} \to 0$ in the equalities (37) and (38) and (40) and (41). Of course, as expected, the expressions of $u_{Nsp}(y,t)$ and $u_{Nst}(y,t)$ given by Equations (43) and (44) are identical to those of $u_{sp}(y,t)$, $u_{st}(y,t)$ from [17] of its Equations (41) and (42).

4. Results and Discussion

In the present study, two unsteady motions of the incompressible UCM fluids through a porous plate channel are analytically studied. Exact expressions for the dimensionless velocity and shear stress fields are determined in a simple way using only finite Fourier sine transform. The solutions corresponding to the oscillatory motion are presented as sums of steady-state and transient components. These are important for the experimentalists who want to eliminate the transients from their experiments. As a check of their correctness, the steady-state components of the velocity field $u_{sp}(y,t)$ and of the non-trivial shear stress $\tau_{sp}(y,t)$ are presented in different forms whose equivalence is graphically shown in Figures 1 and 2. In addition to this, as expected, the known solutions corresponding to incompressible Newtonian fluids performing the same motions are obtained as limiting cases of the present results.

To obtain some physical insight of the results that have been here obtained, Figures 3–7 depict for different values of physical parameters and the time t. In Figure 3 the diagrams of the velocity fields $u(y,t)$ and $u_N(y,t)$ given by Equations (21) and (23), respectively, are together presented for $K = 1$, $\mathrm{Re} = 100$, $\mathrm{We} = 0.002$, 1 and 6 and two distinct values of the time t. In all cases, the fluid velocity decreases from maximum values on the moving plate to the zero value on the stationary wall and the boundary conditions are clearly satisfied. As expected, it is an increasing function with respect to time t. Furthermore, the fluid velocity reduces for increasing values of the Weissenberg number. Consequently, the Newtonian fluids flow faster as compared to the incompressible UCM fluids. It is in accordance with the physical expectation as this number represents the ratio of elastic forces to viscous forces [27]. At the same elastic properties of the fluid, an increase of the Weissenberg number We means a decrease of viscous forces and therefore, the fluid velocity increases. In addition, the convergence of the velocity field $u(y,t)$ to $u_N(y,t)$ when $\mathrm{We} \to 0$ is graphically illustrated too.

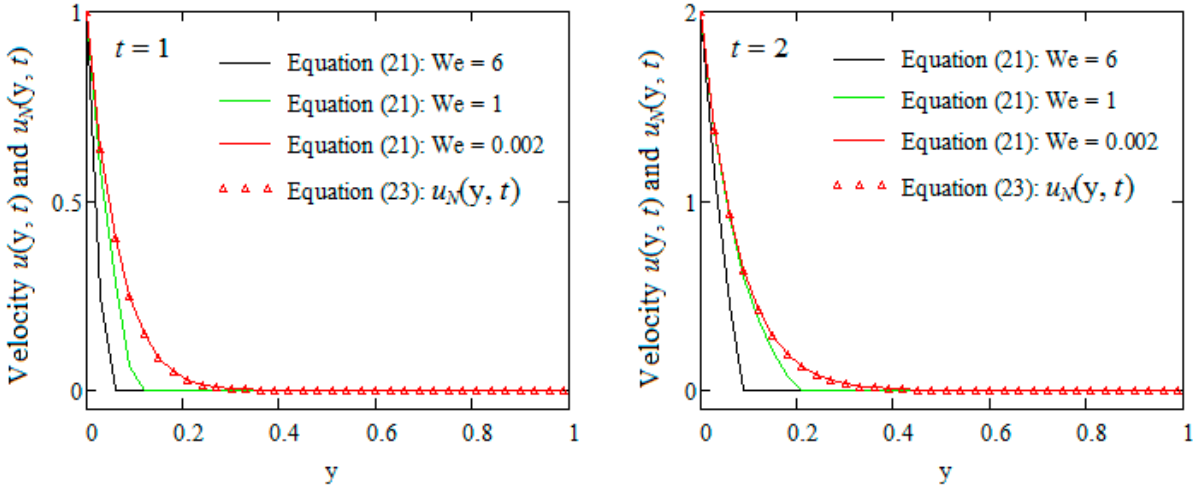

Figure 3. Profiles of the velocity fields $u(y,t)$ and $u_N(y,t)$ respectively given by Equations (21) and (23) for $K = 1$, $\mathrm{Re} = 100$, $\mathrm{We} = 0.002$, 1 and six and two values of t.

The required time to reach the steady-state for the oscillatory motion of the UCM fluids due to the sinusoidal boundary velocity is graphically presented in Figures 4 and 5 for $K = 1$, Re $= 100$, $\omega = \pi/12$ and We $= 0.7$ or 1.5, respectively Re $= 100$, We $= 0.7$, $\omega = \pi/12$ and $K = 1$ or 2. This is the time after which the diagrams of the starting solution $u_s(y,t)$ identically superpose over those of its steady-state component $u_{sp}(y,t)$ and the fluid flows according to the permanent solution. It is founded that the tabular values (which are not included here) corresponding to the two velocity fields at $t = 5$ and $t = 9$ for We $= 0.7$ and 1.5 respectively and $t = 4$ and 3 when $K = 1$, 2 respectively are identical and the required time to reach the steady-state motion of the incompressible UCM fluids remains an increasing function with respect to the Weissenberg number We whereas it decreases for increasing values of K. Consequently, the steady-state is rather obtained for oscillatory motions of incompressible Newtonian fluids as compared to UCM fluids. At the same time, the presence of a porous medium delays the appearance of the steady-state.

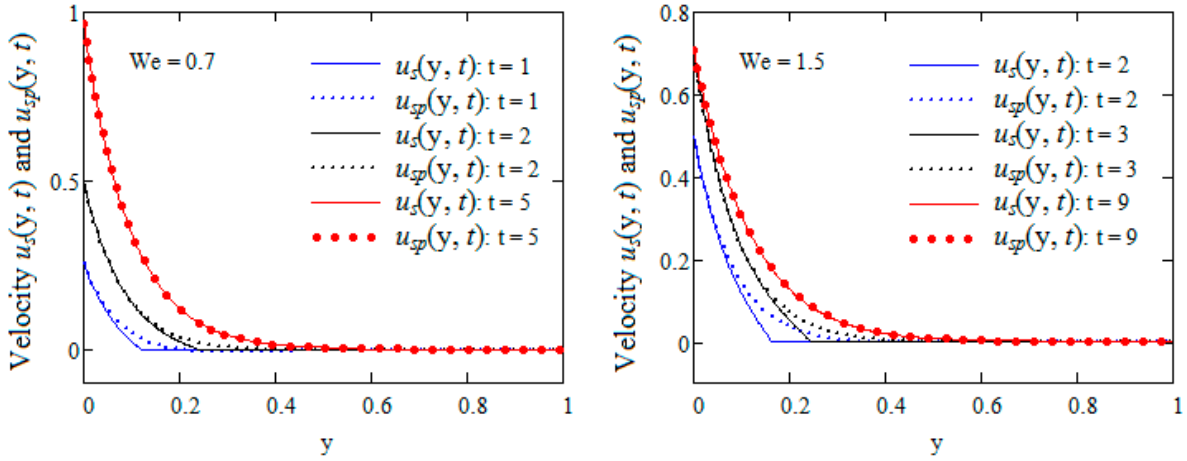

Figure 4. Required time to reach the steady-state for the motion due to the sinusoidal boundary velocity for $K = 1$, Re $= 100$, $\omega = \pi/12$ and We $= 0.7$ and 1.5.

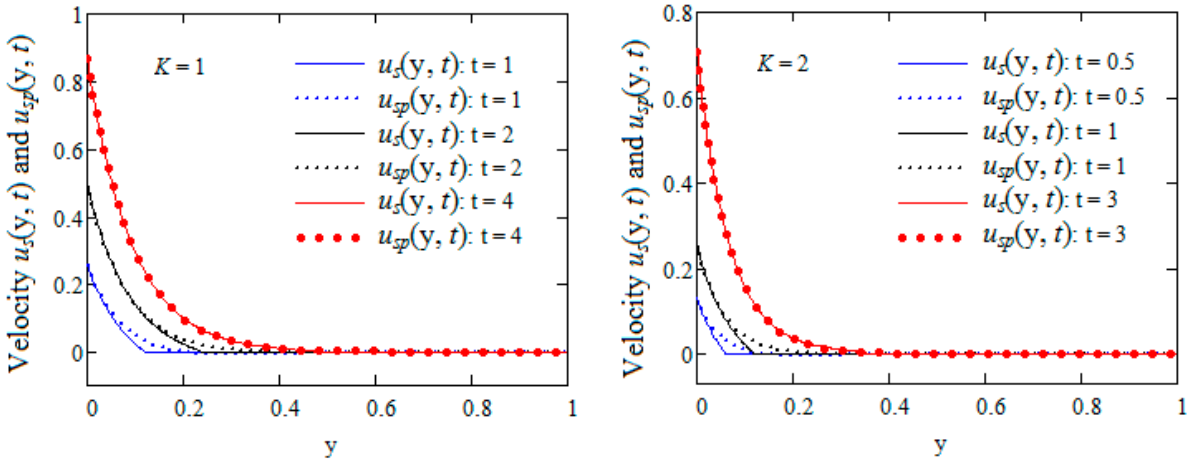

Figure 5. Required time to reach the steady-state for the motion due to the sinusoidal boundary velocity for Re $= 100$, We $= 0.7$, $\omega = \pi/12$ and $K = 1$ and 2.

Figures 6 and 7 present the time variations of the mid plane steady-state velocity and shear stress fields corresponding to the sinusoidal boundary velocity for $K = 0.5$ and 0.8 and four distinct values of the Weissenberg number We. In all cases, the convergence of the general solutions $u_{sp}(0.5,t)$ and $\tau_{sp}(0.5,t)$ to the Newtonian solutions corresponding to We $= 0$ and the oscillatory specific features of the fluid motion are more clearly visualized. The oscillations' amplitude is an increasing function with respect to the Weissenberg

number and slightly diminishes for rising values of K. In addition, as expected, the values of the two entities $u_{sp}(0.5, t)$ and $\tau_{sp}(0.5, t)$ have opposite signs at the same values of the time t.

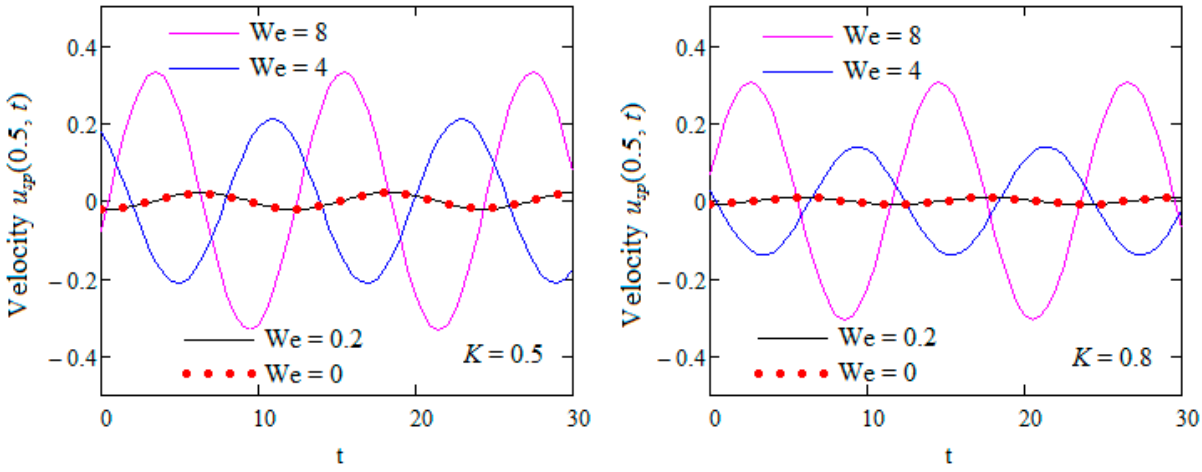

Figure 6. Time variation of the mid plane steady-state velocity $u_{sp}(0.5, t)$ given by Equation (36) for Re $= 100$, $\omega = \pi/6$, $K = 0.5$ and 0.8 and different values of We.

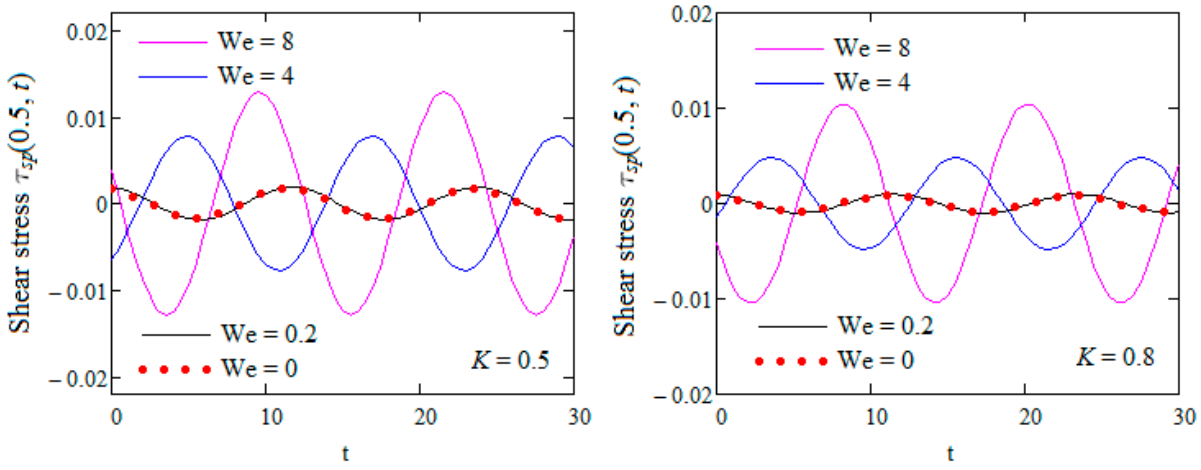

Figure 7. Time variation of the mid plane steady-state shear stress $\tau_{sp}(0.5, t)$ given by Equation (42) for Re $= 100$, $\omega = \pi/6$, $K = 0.5$ and 0.8 and different values of We.

5. Conclusions

Exact expressions are established for the non-dimensional velocity and the shear stress fields corresponding to unsteady motions of the incompressible UCM fluids in-duced by a constantly accelerating or oscillating wall through a porous plane channel. These expressions are easily particularized to get similar solutions for incompressible Newtonian fluids performing the same motions. The influence of physical parameters on the fluid motion as well as the required time to reach the steady-state for the oscil-latory motion are graphically brought to light. It is found that Newtonian fluids flow faster than Maxwell fluids, and the presence of a porous medium slows down the fluid motion. The steady-state is obtained for oscillatory motions of Newtonian fluids as compared to Maxwell fluids. In addition, the presence of a porous medium delays the appearance of this state. The oscillations' amplitude increases or slightly diminishes for increasing values of the Weissenberg number (We) and the porosity parameter K, respectively. Finally, it is worth pointing out the fact that the present results can be ex-tended to incompressible Oldroyd-B or Burgers fluids. Both porous and magnetic ef-fects can be taken into consideration.

Author Contributions: Conceptualization, C.F.; Methodology, C.F.; Validation, R.E.; Writing—review & editing, S.M.S. All authors have read and agreed to the published version of the manuscript.

Funding: This research received no external funding.

Institutional Review Board Statement: Not applicable.

Informed Consent Statement: Not applicable.

Data Availability Statement: Data sharing is not applicable to this article.

Conflicts of Interest: The authors declare no conflict of interest.

Nomenclature

p	pressure
S	extra-stress tensor
T	Cauchy stress tensor
v	velocity
$R(y,t)$	Darcy's resistance
U	characteristic velocity
K	modified permeability
$\tau(y,t)$	shear stress
t	time
k	permeability
ω	frequency of the oscillation
x,y,z	Cartesian coordinate
$\mathbf{e}_x$	is the unit vector
λ	relaxation time
μ	viscosity
ρ	fluid density
φ	porosity
We	Weissenberg number

References

1. Schlichting, H. *Boundary Layer Theory*; McGraw-Hill: New York, NY, USA, 1960.
2. Wang, C.Y. Exact solutions of the unsteady Navier-Stokes equations. *Appl. Mech. Rev.* **1969**, *42*, 270–282. [CrossRef]
3. Wang, C.Y. Exact solutions of the steady-state Navier-Stokes equations. *Annu. Rev. Fluid. Mech.* **1991**, *23*, 159–177. [CrossRef]
4. Erdogan, M.E. On the unsteady unidirectional flows generated by impulsive motion of a boundary or sudden application of a pressure gradient. *Int. J. Non Linear Mech.* **2002**, *37*, 1091–1106. [CrossRef]
5. Rajagopal, K.R. A note on unsteady unidirectional flows of non-Newtonian fluid. *Int. J. Non Linear Mech.* **1982**, *17*, 369–373. [CrossRef]
6. Siddiqui, A.M.; Hayat, T.; Asghar, S. Periodic flows of a non-Newtonian fluid between two parallel plates. *Int. J. Non Linear Mech.* **1999**, *34*, 895–899. [CrossRef]
7. Wang, S.; Li, P.; Zhao, M. Analytical study of oscillatory flow of Maxwell fluid through a rectangular tube. *Phys. Fluids* **2019**, *31*, 063102.
8. Sun, X.; Wang, S.; Zhao, M. Oscillatory flow of Maxwell fluid in a tube of isosceles right triangular cross section. *Phys. Fluids* **2019**, *31*, 123101.
9. Wenchang, T.; Wenxiao, P.; Mingyu, X. A note on unsteady flows of a viscoelastic fluid with the fractional Maxwell model between two parallel planes. *Int. J. Non Linear Mech.* **2003**, *38*, 645–650. [CrossRef]
10. Qi, H.; Xu, M. Unsteady flow of viscoelastic fluid with fractional Maxwell model in a channel. *Mech. Res. Commun.* **2007**, *34*, 210–212. [CrossRef]
11. Qi, H.; Liu, J.G. Some duct flows of a fractional Maxwell fluid. *Eur. Phys. J. Spec. Top.* **2011**, *193*, 71–79. [CrossRef]
12. Al-Hadhrami, A.K.; Elliot, L.; Ingham, D.B.; Wen, X. Flow through horizontal channels of porous materials. *Int. J. Energy Res.* **2003**, *27*, 875–889. [CrossRef]
13. Cimpean, D.; Pop, I.; Ingham, D.B.; Merkin, J.H. Fully developed mixed convection flow between inclined parallel plates filled with a porous medium. *Transp. Porous Med.* **2009**, *77*, 87–102. [CrossRef]
14. Kesavaiah, D.C.; Satyanarayana, P.V.; Sudhakaraiah, A. Effects of radiation and free convection currents on unsteady Couette flow between two vertical parallel plates with constant heat flux and heat source through porous medium. *Int. J. Eng. Res.* **2013**, *2*, 113–118.
15. Marušić-Paloka, E.; Pažanin, I.; Radulović, M. On the Darcy-Brinkman-Boussinesq flow in a thin channel with irregularities. *Transp. Porous Media* **2020**, *131*, 633–660. [CrossRef]

16. Ehlers, W. Darcy, Forchheimer, Brinkman and Richards: Classical hydromechanical equations and their significance in the light of the TPM. *Arch. Appl. Mech.* **2020**. [CrossRef]
17. Fetecau, C.; Narahari, M. General solutions for hydromagnetic flow of viscous fluids between horizontal parallel plates through porous medium. *J. Eng. Mech.* **2020**, *146*, 04020053. [CrossRef]
18. Fetecau, C.; Agop, M. Exact solutions for oscillating motions of some fluids with power-law dependence of viscosity on the pressure. *Ann. Acad. Rom. Sci. Ser. Math. Appl.* **2020**, *12*, 295–311.
19. Danish, G.A.; Imran, M.; Fetecau, C.; Vieru, D. First exact solutions for mixed boundary value problems concerning the motions of fluids with exponential dependence of viscosity on pressure. *AIP Adv.* **2020**, *10*, 065206. [CrossRef]
20. Ullah, H.; Lu, D.; Siddiqui, A.M.; Haroon, T.; Maqbool, K. Hydrodynamical study of creeping Maxwell fluid flow through a porous slit with uniform reabsorption and wall slip. *Mathematics* **2020**, *8*, 1852. [CrossRef]
21. Karra, S.; Prusa, V.; Rajagopal, K.R. On Maxwell fluids with relaxation time and viscosity depending the pressure. *Int. J. Non Linear Mech.* **2011**, *46*, 819–827. [CrossRef]
22. Khan, M.; Malik, R.; Anjum, A. Exact solutions of MHD second Stokes flow of generalized Burgers fluid. *Appl. Math. Mech. Engl. Ed.* **2015**, *36*, 211–224. [CrossRef]
23. Housiadas, K.D. An exact analytical solution for viscoelastic fluids with pressure-dependent viscosity. *J. Nonnewton. Fluid Mech.* **2015**, *223*, 147–156. [CrossRef]
24. Menon, E.S. Fluid flow in pipes. In *Transmission Pipeline Calculations and Simulations Manual*; Elsevier Inc.: Amsterdam, The Netherlands, 2015; Chapter 5, pp. 149–234.
25. Sneddon, I.N. *Fourier Transforms*; McGraw-Hill Book Company, Inc.: New York, NY, USA, 1951.
26. Fetecau, C.; Rauf, A.; Qureshi, T.M.; Mehmood, O.A. Permanent solutions for some motions of UCM fluids with exponential dependence of viscosity on the pressure. *Eur. J. Mech. B/Fluids* under review.
27. Poole, R.J. The Deborah and Weissenberg numbers. *Rheol. Bul.* **2012**, *53*, 32–39.